Regulation of biological processes by intrinsically chiral engineered materials

Baojin Ma, Alberto Bianco

Regulation of biological processes by intrinsically chiral engineered materials

Baojin Ma[1,*] *and Alberto Bianco*[2,*]

[1]Department of Tissue Engineering and Regeneration, School and Hospital of Stomatology, Cheeloo College of Medicine, Shandong University & Shandong Key Laboratory of Oral Tissue Regeneration & Shandong Engineering Laboratory for Dental Materials and Oral Tissue Regeneration & Shandong Provincial Clinical Research Center for Oral Diseases, Jinan, Shandong, 250012, China
Email: baojinma@sdu.edu.cn

[2]CNRS, Immunology, Immunopathology and Therapeutic Chemistry, UPR3572, University of Strasbourg, ISIS, Strasbourg, 67000, France
Email: a.bianco@ibmc-cnrs.unistra.fr

Chirality has a key role in the synthesis of biomolecules and the development of life. Although the effects of many chiral molecules or materials on biological processes have been studied for over 150 years, research aimed at understanding the relationship between the intrinsic chirality of engineered materials and bioresponses is still at the beginning. In this Perspective article, we present three classes of intrinsically chiral engineered materials: carbon dots, metal-based materials and patterned geometries. We elaborate on these chiral materials in terms of design, structural and functional differences between the enantiomers and effects of intrinsic chirality on biological processes. Finally, we address the safety concerns, challenges, opportunities and directions for future development of intrinsically chiral materials.

Introduction

Chiral materials mediate many natural and synthetic processes, including self-assembly1–3, asymmetric reactions4–6, enantioselective catalysis7,8, polarization processes9 and biological responses10–14. In view of the wide application opportunities, engineered materials with intrinsic chiral properties are gaining a lot of interests in many fields15–17. In the biomedical domain, however, chiral materials are still rarely explored or understood, and those that are used usually derive their chirality from surface modifications with chiral entities rather than from intrinsic chirality of the materials themselves14,18–21. These chiral surface modifications usually have the leading role in regulating biological processes, consequently covering up any effects of the intrinsic chirality of the structure.

Chirality exists in all forms of nature and has fundamental roles in living organisms. Amino acids, proteins, carbohydrates, DNA, organelles and more complex tissues and organs all possess chiral characteristics13,22–24, although it is still unknown why almost all proteins composed of l-amino acids are left-handed (levo, l or L, anticlockwise), whereas the DNA double helix structure and most carbohydrates are right-handed (dextro, d or D, clockwise). Minerals in bone tissues, pteropod shells, whale tusks and snail shells are also characterized by chiral hierarchical structures25–27. The natural chirality in biomolecules and biostructures provides unlimited possibilities to interact with engineered chiral materials. Biological processes, including biomolecule structural changes, protein corona formation, cell uptake, cell adhesion, cellular morphological changes, stem cell differentiation, immune response, cancer cell death, nerve repair, antibacterial effects and plant growth regulation, can respond differently to the two enantiomers of engineered materials (Fig. 1). For example, chiral carbon dots (CDs) can mimic topoisomerase I (Topo I) and enantioselectively mediate the topological rearrangement of supercoiled DNA10, and gold enantiomeric nanoparticles (NPs) show different cellular uptake behaviours depending on chiral morphology16.

Before the biological impacts can be studied, materials with asymmetric features must be prepared. One approach to making chiral materials exploits chiral precursors that do not racemize during the

synthesis28–31, most popularly amino acids or peptides such as cysteine29, serine31, glutamic acid21,32, aspartic acid33, glutathione16 and Cys-Phe dipeptide34. Alternatively, chirality can be triggered in a material by physical methods, such as applying polarized light in the presence of chiral molecules35. As a representative example, the two enantiomers of Au NPs were synthesized in the presence of the Cys-Phe dipeptide under polarized light irradiation. Nanofabrication has also enabled a whole new range of materials, including polymers, glass and quartz, to be patterned with chiral geometries that show interesting prospects in regulating biological processes36. For example, chiral Archimedean spiral geometries (ASGs) showed the ability to regulate stem cell differentiation37. It is worth noting that most current studies lack a detailed comparison between the two enantiomeric forms of the same material, making it difficult to understand the role of chirality in the biological processes36,38–40.

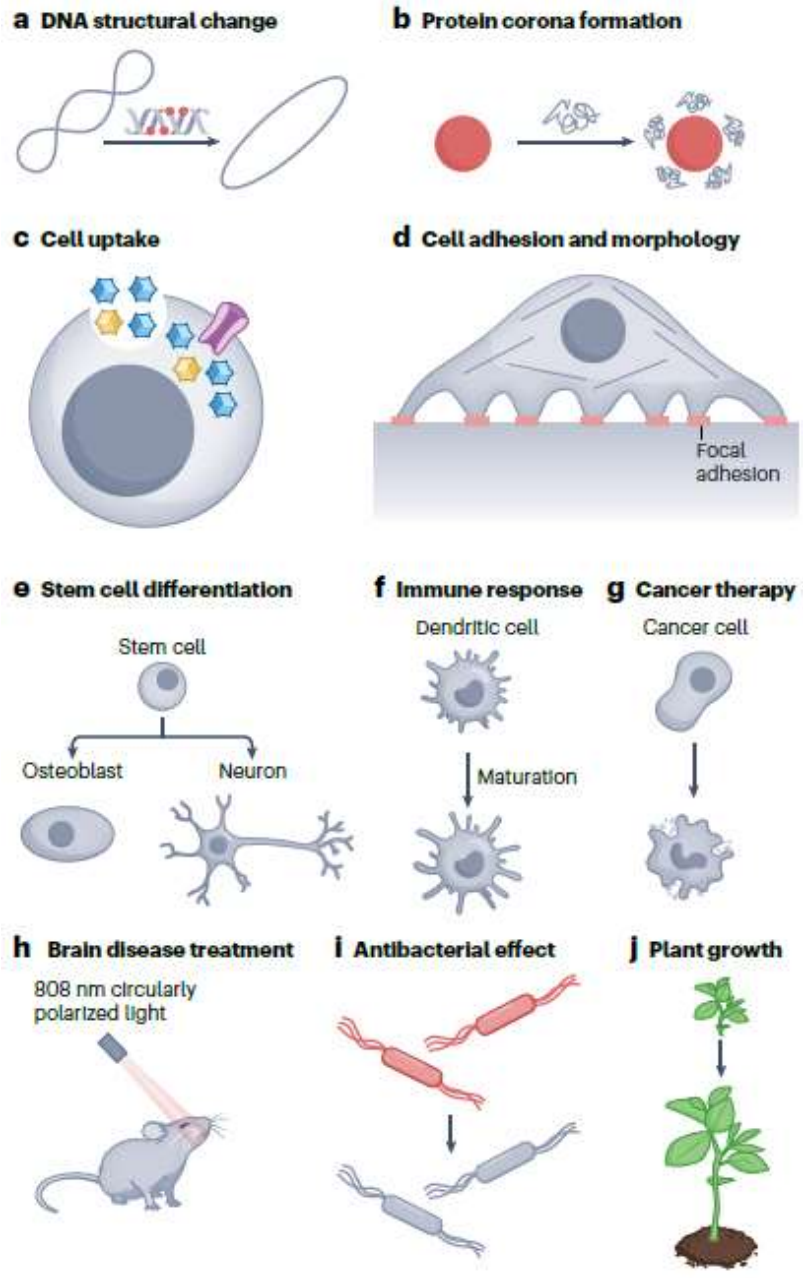

Fig. 1 | Various biological processes that can be regulated by chirality. a, Structural change of a biomolecule. b, Protein corona formation. c, Cell uptake. d, Cell adhesion and morphology. e, Stem cell differentiation, such as osteogenic and neural differentiation. f, Immune response mediated by the enhanced maturation of dendritic cells. g, Cancer cell death in cancer therapy. h, Nerve repair in brain disease treatment. i, Antibacterial effect. j, Plant growth.

In this Perspective article, we discuss intrinsically chiral materials, covering their design, the differences in structure and function between the enantiomers and the effects of the chirality of the material on biological responses and processes. The intrinsically chiral engineered materials are divided into three classes on the basis of the components and design methods to obtain them, comprising CDs, metal-based materials (MBMs) and patterned geometries. The definitions we use for different types of chirality are reported in Box 1. We hope that this Perspective article will be beneficial to build a bridge between fundamental research and future clinical applications and to promote further the development of chiral medicine mediated by materials as alternative drugs41,42.

BOX 1

Definitions of chiral materials and categorization

Although the concept of chirality was discovered by Louis Pasteur more than 150 years ago24, we cannot apply the traditional definition of chirality to the current materials because the two enantiomers cannot be clearly identified with left-handedness or right-handedness using the classical analytical techniques (X-ray crystallography, optical rotation and circular dichroism).

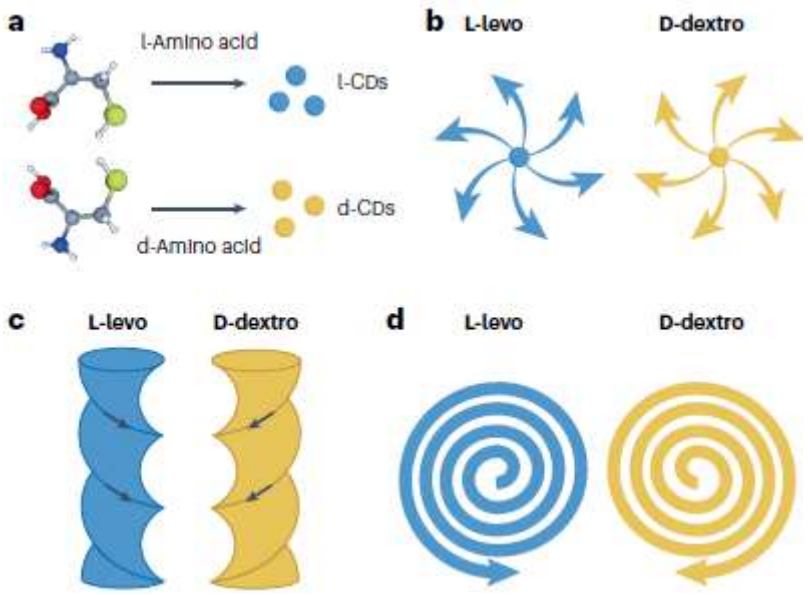

In the available literature, there is still no coherence between the chiral structures and the starting chiral precursors. In addition, some chiral nanoparticles visualized by microscopic techniques (such as transmission electron microscopy or scanning electron microscopy) do not necessarily reflect the chirality of the precursors or the molecules used to induce the chirality. To avoid confusion and to provide general descriptors that can be applied in future studies, we use the lowercase letters l (for levo-rotary) and d (for dextro-rotary) to refer to the chirally engineered materials that do not have

observable microstructures or nanostructures by microscopy, mainly carbon dots (CDs) (see the figure, part a). We use capital letters L and D to refer to the chiral engineered materials with microscopy-observable microstructures and nanostructures (see the figure, parts b–d). The chirality in part b of the figure is determined by the direction of the arrows from the centre outwards, and the chirality in part c is determined by the direction of the 3D helical lines from the top downwards, similar to snails and screws. For part d of the figure, the chirality is determined by the direction of Archimedes spirals from the centre outwards.

Intrinsically chiral carbon dots

CDs are particularly attractive because of their simple preparation, low cost, high biocompatibility and biodegradability43–47. CDs can have a wide variety of functional groups on their surface, and their carbon core can be either crystalline or amorphous. Both the surface chemistry and core influence the physicochemical properties of CDs48–50. Their synthesis benefits from an almost infinite number of possible reagents and precursors, including chiral molecules. On the basis of the currently available literature, we can classify chiral CDs into two groups: intrinsically chiral CDs obtained from chiral precursors and chiral CDs modified post-synthesis with chiral molecules. The chirality of the former derives from the chiral centres of the precursors that do not undergo racemization during the synthetic steps and from the hierarchical geometry of the final dots. By contrast, the chiral characteristics of post-synthetically modified chiral CDs mainly come from the surface chiral molecules rather than from the CDs themselves. Therefore, to uncover the effects of the dots on the biological processes, we consider only intrinsically chiral CDs.

Catalytic activity

CDs can be catalytically active51,52, and their chirality can influence catalytic reactions. Chiral CDs obtained from l-serine or d-serine had the inverse handedness of the precursor (as evidenced by high-resolution transmission electron microscopy; Fig. 2a) and showed an enantioselective catalytic activity31. The inversion of chirality of these CDs was attributed to the electrochemical method of preparation, which led to an initial electrooxidation of the hydroxyl group of serine, followed by the formation and polymerization of a well-defined primary structure characterized by two cyclic dipeptides as a spatial structural unit with a c-axis of hexagonal symmetry. It is worth noting that the nomenclature we apply to these chiral dots corresponds to L-levo and D-dextro definitions illustrated in Box 1, maintaining the correlation between the chiral precursors and the derived materials (l-Ser → L-Ser-CDs and d-Ser → D-Ser-CDs), even though the structures in the space and related models have opposite chirality. L-CDs with D-handedness have higher catalytic activity in the oxidation of l-DOPA, whereas D-CDs with L-handedness have higher catalytic activity in the oxidation of d-DOPA

(Fig. 2b). This enantioselective catalytic oxidation of DOPA was owed to the different affinities of each chiral CD to the DOPA enantiomers, proving the effect of the intrinsically chiral structure of the CDs on biological function. In vivo, tyrosinase catalysis converts l-DOPA to dopachrome, a molecule that subsequently spontaneously polymerizes to melanin53. Melanin protects the skin from the damage of UV light, and a deficiency of it can cause skin pathologies54,55. Therefore, L-Ser-CDs with D-handedness have the potential to function as an enzyme mimetic to promote the production of dopachrome and melanin, when the natural process is damaged.

In another study, cysteine-derived chiral CDs (Cys-CDs) mimicked the activity of Topo I, catalysing the geometrical reorganization of supercoiled DNA10 (Fig. 2c). Here, the definition of the chirality refers to l and d precursors because microstructures or nanostructures observable by microscopy are missing. d-Cys-CDs showed faster catalytic activity than l-Cys-CDs in transforming supercoiled plasmid DNA into a nicked open-circular configuration. d-Cys-CDs can strongly intercalate into the DNA double helix, producing hydroxyl radicals that cleave the phosphate backbone in one strand of the double helix. In normal physiological conditions, Topo I relaxes supercoiled DNA by cleaving one strand of the DNA double helix and then re-ligates the nicked sites to trigger the transcription from DNA to RNA56. Similar to Topo I, d-Cys-CDs might affect genetic processes, regulating cellular behaviours and fate.

Interactions with proteins and cells

Understanding the interactions between chiral CDs and proteins and/or cells is still at the beginning, but these interactions hold a lot of interests for their potential to modulate cellular processes, targeting and treating specific diseases. For example, controlling the level of glucose in the blood is critical to treat type 2 diabetes and hyperglycaemia57,58. However, the serious side effects and low efficacy of traditional drugs (such as biguanides, sulfonylureas and α-glucosidase inhibitor) have opened a dilemma in their use59–61. Within the different treatments, inhibiting the activity of maltase (an enzyme that hydrolyses maltose and similar α-glucosides to glucose) can efficiently decrease glucose levels in the blood by preventing hydrolysis. Surprisingly, glutamic acid-derived chiral CDs (Glu-CDs) can regulate the rate of hydrolysis of maltose by maltase32. d-Glu-CDs inhibited the activity of maltase more efficiently than l-Glu-CDs, owing to a structural change in the target protein induced by its interaction with the chiral dots, thereby reducing the level of glucose.

Enantiomers of engineered materials interact with proteins in different ways, which can affect the formation of protein coronas and the rate of cellular uptake of nanomaterials62,63. Enantiomers of chiral CDs might also interact differently with corona proteins. l-Arg-CDs synthesized from l-arginine and (S,S)-1,2-cyclohexanediamine bound substantially worse to human serum albumin, one of the most abundant proteins in the blood, than did d-Arg-CDs synthesized from l-arginine and (R,R)-1,2-

cyclohexanediamine64. The distinct behaviours of the two asymmetric CDs in the process of coronation affected how each material interacted with different (for example, cancer versus immune) cells. Cancer cells (for example, HeLa cells), although they internalized both chiral l-Arg-CDs and d-Arg-CDs more efficiently than achiral Arg-CDs, were not more sensitive to one enantiomer over the other, particularly in serum medium (serum is responsible for protein corona formation). However, human immune cells (for example, THP-1-derived macrophages) took up more l-Arg-CDs than d-Arg-CDs, whether in a serum or serum-free medium. The protein corona usually reduces the uptake of nanomaterials by cells65, which was also the case with the chiral and achiral Arg-CDs. The difference in overall chiral CD uptake between cancer cells and immune cells might have interesting implications in cancer therapy. After intravenous injection of the two CD enantiomers and protein corona formation in the blood, immune cells internalized fewer d-Arg-CDs compared with l-Arg-CDs, leaving more of the d-enantiomer for cancer cells to take up and contributing to the accumulation of d-Arg-CDs at the tumour site. If the chiral dots are endowed with anticancer properties, this behaviour would result in more efficient cancer therapy.

Chiral dot enantiomers internalized differently in cells can regulate intracellular processes differently. Chiral CDs internalized by human bladder epithelial cells were able to regulate the energy of cellular metabolism, which is crucial to maintain essential cellular functions. l-Cys-CDs showed a higher dose-dependent and time-dependent enhancement in cellular glycolysis in comparison to d-Cys-CDs66 (Fig. 2d). Neither l-Cys-CDs nor d-Cys-CDs affected the mitochondrial respiration and the ATP level, confirming the high biocompatibility of chiral CDs. Although the mechanism of regulating glycolysis was not studied, it is worth noting that both l-Cys-CDs and d-Cys-CDs had similar internalization behaviour and intracellular distribution, opposite to the results of chiral CDs made of arginine64. We can presume that both the type of chiral precursor and the physicochemical properties (such as size, charge, elemental doping and surface functional groups) of the obtained chiral CDs affect how they are internalized in the cell and influence intracellular processes. Despite this evidence, it is still too early to rationally design alternative chiral CDs with the desired cell penetration capacities.

On the basis of the effects found so far on protein and cell functions, the bioapplications of chiral CDs are rapidly expanding. It has been confirmed that chiral CDs can regulate enzymatic activity67,68. l-Glu-CDs and d-Glu-CDs, synthesized from glutamic acid in the presence of citric acid, were coassembled with GOx69 (Fig. 2e). Although both chiral enantiomers enhanced the activity of GOx, d-Glu-CDs did so more efficiently because of their higher affinity towards the protein and the slight changes induced on the secondary structure of GOx. Although the content of α-helix decreased after binding of the chiral dots, the content of β-strands increased, exposing more of the redoxactive centres of the protein and eventually enhancing its catalytic activity. As the protein–CD complexes were easily internalized by cancer cells, the d-enantiomer generated more hydrogen peroxide than the l-enantiomer, provoking an extensive cell death and restraining the tumour growth in vivo. The

same chiral l-Glu-CDs and d-Glu-CDs were linked to ovalbumin (OVA) to form the corresponding complexes (l-OVA and d-OVA) for cancer immune therapy70. d-OVA was better internalized than l-OVA by mouse bone-marrow-derived dendritic cells (BMDCs), triggering higher expression of co-stimulatory molecules (such as CD80, CD86 and tumour necrosis factor) and higher BMDC maturation. d-Glu-CDs devoid of OVA could also promote the maturation of BMDCs to a certain extent, whereas l-Glu-CDs or OVA alone almost failed. Thus, d-OVA showed a remarkable in vivo activity against tumour growth compared with l-OVA and OVA alone. Importantly, this kind of chiral dot augmented the percentage of CD8+, CD4+ and CD8+CD4+ T cells in the lymph nodes and infiltrated more cytotoxic T lymphocytes to the tumour tissue, ultimately increasing the antitumoural efficiency. Therefore, chiral CDs have potential as adjuvants to achieve an enhanced immunological antitumour effect.

In an environmental context, chiral CDs might influence plant seeding and growth71. d-Cys-CDs improved the root vigour and growth of mung bean plant better than l-Cys-CDs in a dose-dependent manner (Fig. 2f). The difference originates from the interactions between each enantiomer and proteins, in particular the enzymes involved in the respiratory chain photosynthesis of the plant.

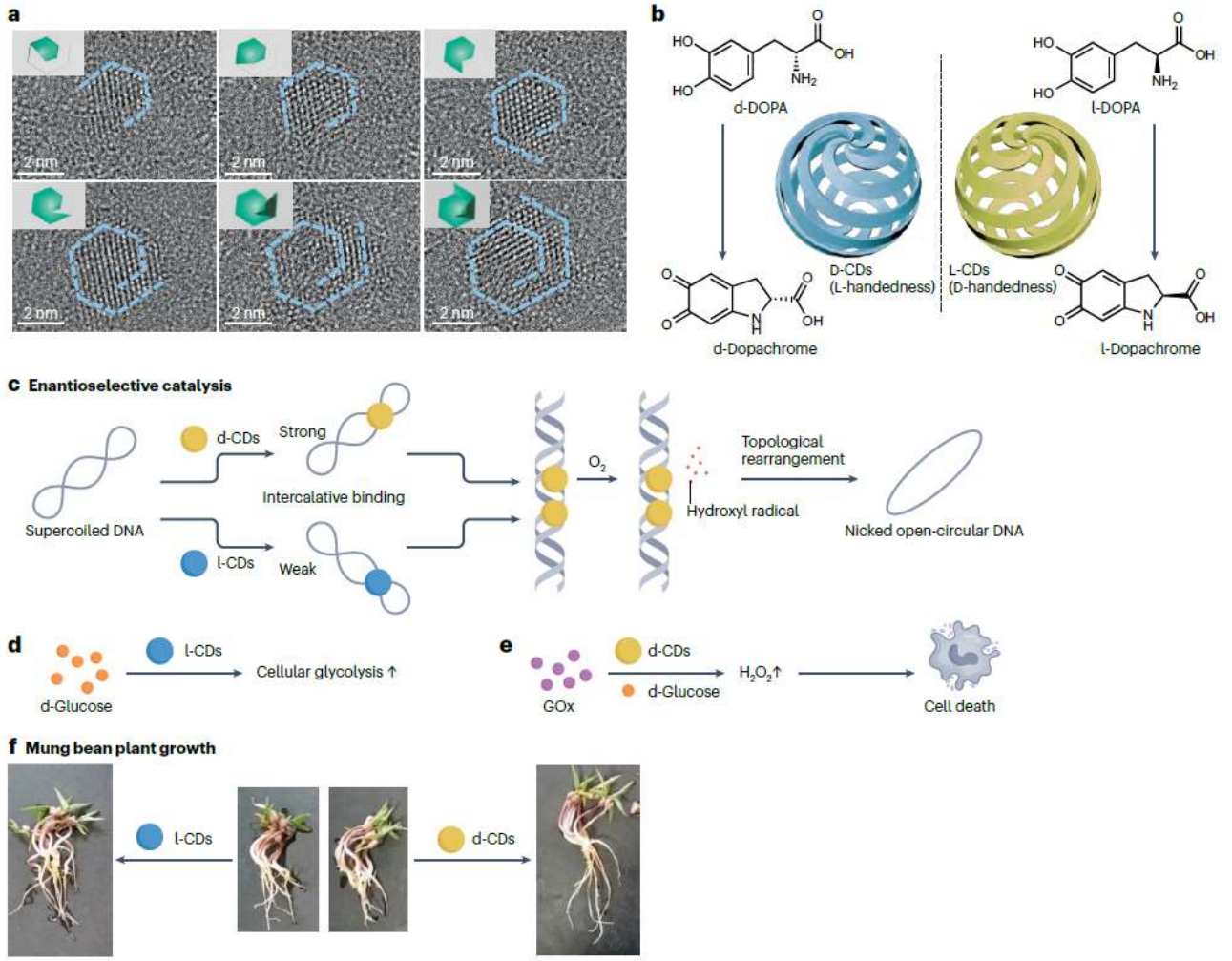

Fig. 2 | Chiral carbon dots regulating various biological processes. a, Growth direction of chiral carbon dots (CDs), showing serial angle changes in the lattice arrangement, corresponding to the focal plane change. b, Enantioselective catalytic activity of chiral CDs. L-CDs with D-handedness selectively catalyse l-DOPA to l-dopachrome, whereas D-CDs with L-handedness selectively catalyse d-DOPA to d-dopachrome. c, Topological rearrangement of supercoiled DNA by enantioselective catalysis mediated by chiral CDs. Cys-CDs possess a topoisomerase I-like activity and can catalyse the transformation of supercoiled plasmid DNA into a nicked open-circular configuration, induced by the formation of hydroxyl radicals. d-Cys-CDs show higher enzyme-like activity than l-Cys-CDs owing to the stronger intercalation into DNA double helix. d, l-Cys-CDs upregulate cellular glycolysis, whereas d-Cys-CDs have no influence. e, Chiral CDs regulating glucose oxidase (GOx) activity. Both chiral CDs can substantially enhance the activity of GOx, d-Glu-CDs more efficiently than l-Glu-CDs. By the efficient delivery of GOx to cancer cells, the complex of d-Glu-CDs, rather than the l-enantiomer or GOx alone, can lead to the generation of a higher level of intracellular hydrogen peroxide by catalysing the decomposition of d-glucose, eventually causing cancer cell death and tumour growth inhibition. f, Effects of chiral CDs on bean plant growth. d-Cys-CDs enhance photosynthesis better and accumulate more carbohydrate in mung bean plants than l-Cys-CDs by promoting the root vigour and the activity of Rubisco enzymes. Panels a and b adapted with permission from ref. 31. Copyright 2022 American Chemical Society. Panel f adapted with permission from ref. 71, Royal Society of Chemistry.

Antibacterial activity

Chiral CDs are also finding applications as antibacterial agents. Chiral Cys-CDs showed antibacterial efficiency against Micrococcus luteus, Bacillus subtilis, Klebsiella aerogenes, Burkholderia thailandensis and Escherichia coli72. d-Cys-CDs were more lethal to M. luteus, B. subtilis and E. coli. Inversely, the l-enantiomer performed better against K. aerogenes. Both enantiomers were similarly efficient in inhibiting B. thailandensis. Although this difference in antibacterial efficiency could possibly be ascribed to the specific interaction between each chiral CD and intracellular proteins, more studies should be performed using other types of chiral dots and bacterial strains to understand the mechanisms behind the antibacterial activity of chiral CDs.

Intrinsically chiral metal-based materials

MBMs (made of pure or mixed elements, or made of their oxide or sulfide forms) possess unique physicochemical properties (such as superparamagnetism and photocatalytic activity), and they can also adopt chiral structures. Similar to chiral CDs, MBMs can be made chiral by being directly combined with chiral molecules28,29,34,72. In addition, chiral MBMs can be grown by applying polarized light to metal seeds in the presence of chiral molecules34,73. We underline an obvious difference between chiral MBMs and chiral CDs: although most chiral MBMs display observable chiral

structures (such as chiral propellers, nanooctopods, fan-like nanostructures and helical pointed stars) by scanning electron microscopy or transmission electron microscopy, the chirality of CDs is usually only proven by circular dichroism spectra, being nanostructures that are difficult to visualize. In the biomedical context, chiral MBMs have been explored so far for molecular detection, cancer cell discrimination, immune regulation, cancer therapy, antiviral and antibacterial applications and treatment of brain diseases (for example, Alzheimer and Parkinson diseases). Strategies to control the morphology of gold nanomaterials have reached a high degree of maturity73, providing ample opportunities to prepare Au enantiomeric NPs74. Chiral plasmonic Au nanopropellers were synthesized using seeded growth by a chiral ligand75. These particular structures grew on the tips of Au nanotriangles in the presence of l-Cys or d-Cys. Owing to their different binding energies with chiral biomolecules, the two nanopropeller enantiomers were able to differentiate the chirality of biomolecular enantiomers (l-DOPA, l-carnitine, d-carnitine and doxorubicin) on the basis of the change in surface-enhanced Raman scattering spectra after nanopropeller–biomolecule complexation (Fig. 3a). Chiral Au nanomaterials have also been found to have different cellular uptake behaviours; Au NPs with L-handedness are internalized to a higher extent than the specular enantiomers16,34.

Immune regulation

Chiral Au NPs are emerging as possible adjuvants to regulate immune responses12. Chiral Au NPs with controllable nanometre-scale chirality and high optical anisotropy factor were generated under irradiation with circularly polarized light35. L-Au NPs have a higher affinity to the adhesion G-protein-coupled receptors (for example, CD97) and epidermal growth factors (for example, epidermal-growth-factorlike- module receptor 1) present at the membranes of dendritic cells and can be transported into the cells by endocytosis better than D-Au NPs (Fig. 3b). Internalized chiral Au NPs open the potassium-efflux channels, activate the NLRP3 inflammasome, induce the production of cytokines and increase the expression of co-stimulatory molecules for the activation of T cells. These properties were used in a vaccination protocol, in which L-Au NPs were more efficient than the right-handed enantiomer as adjuvants against the H9N2 influenza virus. It is well known that an enhanced immune response is helpful to cancer immunotherapy. Besides T cells, natural killer cells are also efficiently activated by the chiral Au NP-enhanced maturation of dendritic cells. L-Au NPs can induce more T and natural killer cells than can D-Au NPs both in vitro and in vivo73 (Fig. 3c). In this context, L-Au NPs were more efficient at triggering apoptosis in tumour cells and prolonged the survival of mice compared with D-Au NPs. L-Au NPs also had a bigger mechanical force of interaction with dendritic cells than D-Au NPs, thus stimulating the cells more efficiently and providing a stronger immune response against cancer as immunoadjuvants.

Brain disease treatment

The same chiral Au NPs used as adjuvants have been used to tackle brain diseases. In particular, they are capable of promoting the neuron differentiation of mouse neural stem cells34,76 (Fig. 3d). Similar to the adjuvant study, L-Au NPs were about twice as efficient as D-Au NPs in promoting neural stem cell differentiation owing to their higher endocytosis efficiency. In addition, under near-infrared irradiation, L-Au NPs could remove almost 70% of amyloid and hyperphosphorylated p-tau proteins, alleviating the symptoms of Alzheimer disease. The other common degenerative brain disease is Parkinson disease77. Because the proteins (such as tyrosinase and Cu−Zn superoxide dismutase) involved in the onset of this pathology interact with copper ions, Cu-based chiral NPs might have positive repercussions on fibre formation, combined with their activity as reactive oxygen species (ROS) scavengers. L-handed copper oxide (l-CuXO) NPs, mimicking the activities of peroxidases, inhibited neurotoxicity in a cellular model of Parkinson disease and rescued memory loss in a mice Parkinson model40. One of the pathogenic mechanisms in Parkinson disease is the aggregation of α-synuclein from the original physiological monomeric form to the pathological fibres77. ROS generation was used to disaggregate α-synuclein fibrils into short fragments and single oligomers. Under near-infrared irradiation, right-handed CuxCoyS NPs produced more ROS than the l-enantiomer, more effectively disaggregating the pathological fibres78 (Fig. 3e).

Antibacterial activity

Chiral MBMs might also have potential as novel antibacterial agents, particularly in view of the continued emergence of multiresistant bacteria and the appearance of new bacterial strains. Chiral Au nano-bipyramids (NBs) have been tested against bacterial infections79. D-Au NBs possessed higher antibacterial efficiency (killing 98% of Staphylococcus aureus) than L-Au NBs (killing 70% of S. aureus), promoting wound healing and preventing sepsis. D-Au NBs are likely better antibacterial agents because they have a higher binding affinity to protein A, found in the cell wall of S. aureus, than do L-Au NBs; they consequently destroy bacterial cell walls and provoke mechanical deformation of the bacteria to a greater extent. In an alternative strategy that combined the properties of the materials with an external stimulus, chiral cobalt star-like microparticles (MPs) with six points were able to exert strong antibacterial activity under an electromagnetic field, L-Co MPs performing better than D-Co MPs80 (Fig. 3f). Owing to the chiral-induced spin selectivity effect, the transport of electrons was spin-dependent, and more electrons were transferred through D-Co MPs under electromagnetic stimulation. Subsequently, these D-handed MPs produced more singlet oxygen than the L-enantiomer, killing the bacteria more efficiently.

In view of these studies, we expect that chiral materials made of other types of metals (silver, zinc, titanium and so on) will appear in the future, expanding their applications in the biomedical domain.

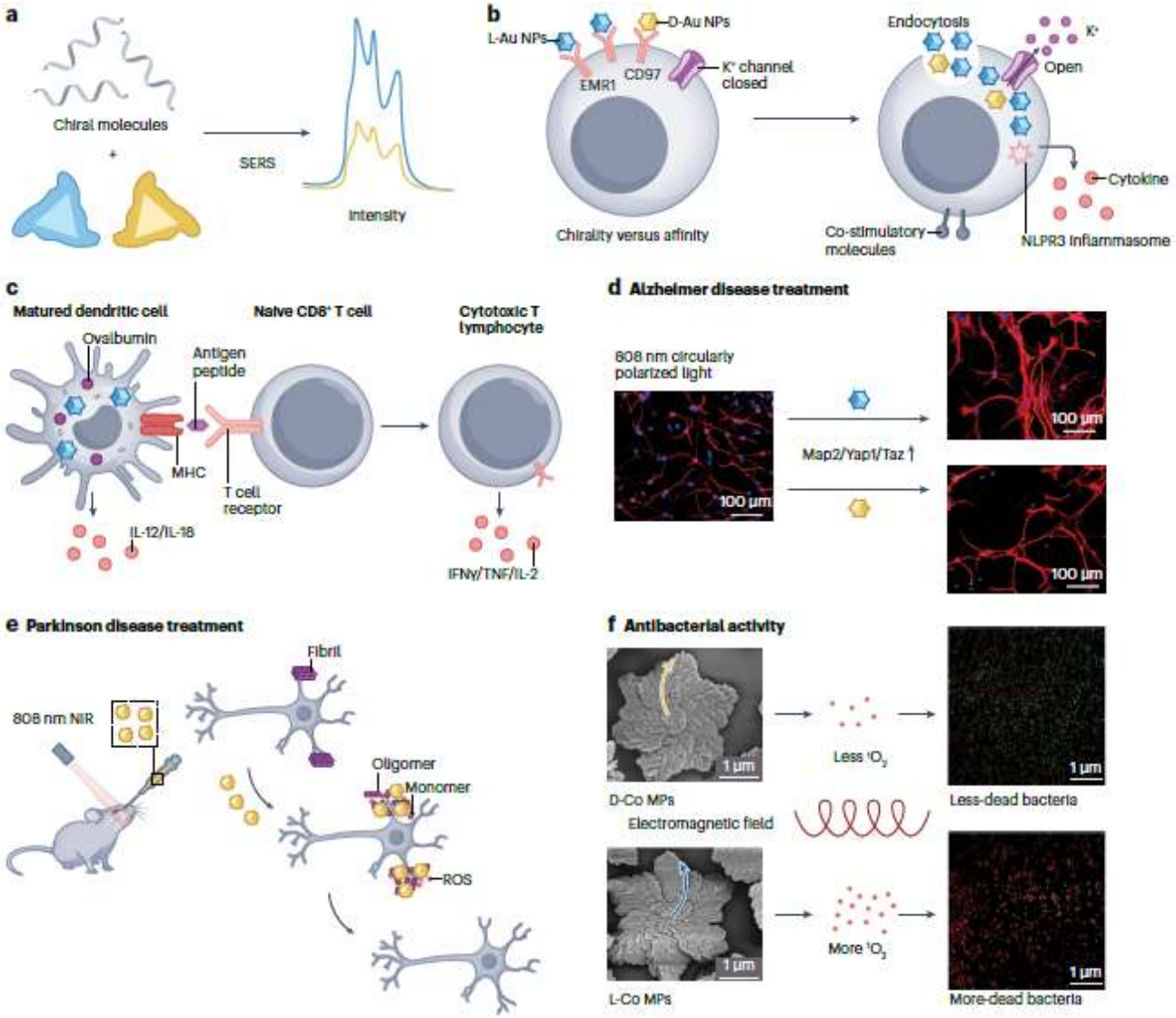

Fig. 3 | Chiral metal-based materials regulating various biological processes. a, Chiral molecule detection. When chiral biomolecules are combined with chiral plasmonic Au nanopropellers, changes in the locations and intensity of the peaks occurred in surface-enhanced Raman scattering (SERS) spectra, enabling differentiation of the chirality of the biomolecules. b, Chiral Au nanoparticles (NPs) activate the immune response by potassium efflux and NLRP3 activation, inducing maturation of bone-marrow-derived dendritic cells and production of cytokines and co-stimulatory molecules to activate T cells. Owing to the higher binding affinity to cells, L-Au NPs possess higher activation efficiency than D-enantiomer. c, Chiral Au NPs for cancer immunotherapy. Chiral Au NPs stimulate dendritic cells to take up antigens and present major histocompatibility complex (MHC) I antigen peptides to activate CD8+ T cells. The activated CD8+ T cells express tumour necrosis factor (TNF) and interferon-γ (IFNγ) and specifically recognize antigen peptides via T cell receptors. Meanwhile, cytokines (IL-12, IL-18 and IL-2) expressed by the activated dendritic cells and T cells enhance the cytotoxic activity of natural killer cells. These processes induce the apoptosis of tumour cells. Given that the force of interaction between L-Au NPs and dendritic cells is higher than that for D-Au NPs,

thus further promoting the activation of natural killer cells and CD8+ T cells and their infiltration into tumour tissue, L-Au NPs showed a greater ability to treat cancer. d, Chiral Au NPs promote neuron differentiation. Under illumination by 808 nm circularly polarized light, L-Au NPs substantially change mechanotransduction signals, better promoting neuron differentiation of mouse neural stem cells than D-Au NPs. e, Chiral CuxCoyS NPs treat Parkinson disease by producing reactive oxygen species (ROS) under near-infrared (NIR) irradiation, leading to disaggregation of α-synuclein fibrils into short fragments and single oligomers. f, Six-pointed star-shaped, chiral Co microparticles (MPs) treat bacterial infections. L-Co MPs can generate more 1O2 under stimulation by an electromagnetic field than D-enantiomer, achieving a better antibacterial efficiency. Panel d adapted from ref. 34, CC BY 4.0. Panel f adapted with permission from ref. 80, Wiley.

Patterned chiral geometries

Advances in nanofabrication have made it possible to pattern chiral geometries onto surfaces of various materials, endowing them with a highly controlled intrinsic chirality that is usually difficult to achieve by traditional solution methods36,81,82. Owing to the unique preparation methods, such as photolithography and focused ion-beam-induced deposition, patterned chiral geometries invite different (bio)applications from those of chiral NPs. Chiral patterns (mainly on metals, quartz and glass) can be used for biosensing and biodetection. When chiral biomolecules adsorb onto the chiral surface, the circular dichroism spectra change, providing information on the type of interacting chiral biomolecule38,83,84 (Fig. 4a,b).

Cellular behaviour regulation

Chiral patterns may be able to instruct cell behaviours. It has been extensively demonstrated that nano-topography or micro-topography of a material regulates cell adhesion, morphology, migration, proliferation and differentiation85–90. Chiral swirled micropatterns with shurikenlike shape were prepared by miniaturizing polyvinyl alcohol stripes on polystyrene discs through photolithography91. Cell focal adhesions and actin filaments organized along the direction of swirling stripes on L-handed or D-handed micropatterns, forming corresponding chiral focal adhesions and cytoskeletal arrangements (Fig. 4c). The cytoskeletal structure affected cellular uptake, and the activation of mechanotransduction signals mediated by focal adhesions could increase DNA synthesis, synergistically promoting gene transfection. The efficiency of this transfection was mainly affected by the swirling angle, without a preferential chirality for L-handedness or D-handedness. Interestingly, rodent primary mesenchymal stem cells migrated more quickly anticlockwise than clockwise on a microstripe geometry, whereas there was no significant difference for fibroblasts or cancer cells, meaning that different types of cells may have different responses to chirality92.

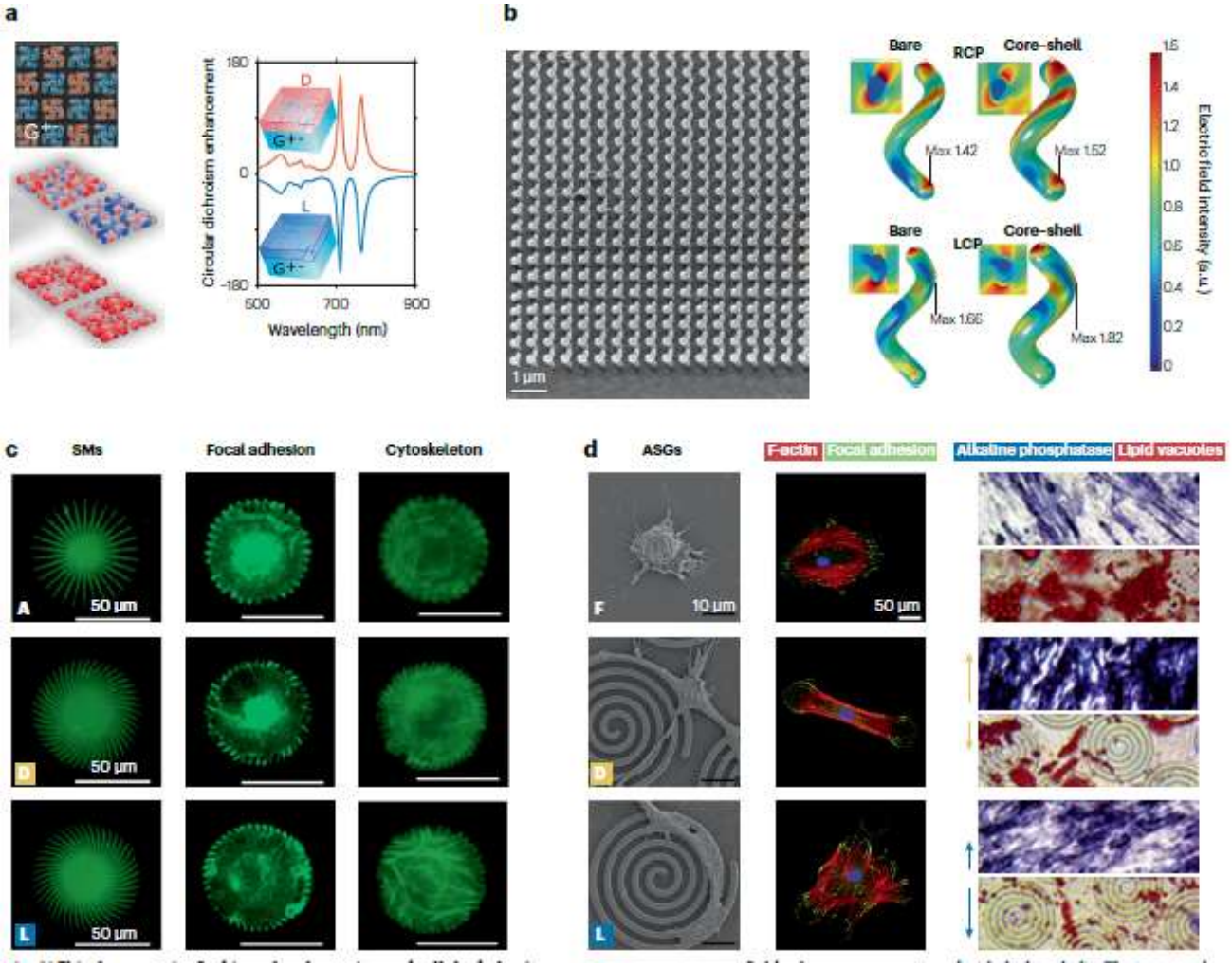

Fig. 4 | Chiral geometries for biomolecule sensing and cellular behaviour regulation. a, Chiral nanoplasmonic arrays and circular dichroism signal enhancement spectra for chiral molecule sensing and detection. The racemic gammadion array G+− shows large optical chirality and electric field enhancement, but no circular dichroism signal. When d-molecular and l-molecular layers are formed on the top of the racemic gammadion array sensor, enhanced circular dichroism spectra with higher sensitivity for chiral detection are obtained. The circular dichroism signal enhancement is calculated from the ratio CDG/CD0, where CDG is the circular dichroism of the racemic sensor with the chiral molecule layers and CD0 is the circular dichroism of only the chiral molecule layers without any nanostructure. b, Chiral Pt-poly-o-phenylediamine core–shell nanohelice array (scanning electron microscopy image) for chiral molecule sensing and detection. The electric field distribution is calculated via numerical simulations by considering the scattering resonance peak for left-handed circularly polarized (LCP) and right-handed circularly polarized (RCP) light, and the core–shell helix presents a near-field enhancement compared with the bare helix. The increased field intensity can more strongly interact with surrounding biomolecules, providing a beneficial contribution to system-sensing capabilities. c, Chiral swirling micropatterns (SMs) regulating the chiralities of focal adhesions and cytoskeleton (A, straight; D, dextro; L, levo). Once the focal adhesions occur, the organization of

actin filaments follows the direction of swirling stripes on L-handed and D-handed micropatterns, forming the corresponding adhesion states and cytoskeletal arrangements. d, Chiral Archimedian spiral geometries (ASGs) regulating stem cell adhesion, morphology and differentiation (F, flat; D, dextro; L, levo). D-ASGs possess higher efficiency for osteogenic differentiation, and L-ASGs and D-ASGs both inhibit adipogenic differentiation. Panel a adapted from permission from ref. 84. Copyright 2018 American Chemical Society. Panel b adapted from permission from ref. 38. Copyright 2021 American Chemical Society. Panel c adapted with permission from ref. 91, Elsevier. Panel d adapted with permission from ref. 37, Elsevier.

Stem cell differentiation

Patterned chiral geometries have also shown their power to regulate the fate of stem cells37,93. Chiral ASGs were patterned on a quartz substrate by traditional photolithography. Stem cells cultured on this substrate showed a stronger response to right-handed ASGs than to left-handed ones37. D-ASGs generated significantly higher cytoskeletal tension by regulating focal adhesion proteins and F-actin compared with the L-enantiomer (Fig. 4d). The parallel bundles of F-actin in human pattern units and form a dumbbell-like structure. By contrast, a woven actin network within surrounding pattern units was observed on L-ASGs. The difference in the organization of the actin cytoskeleton reflected how chirality influences the morphology, cytoskeletal contractility and mechanosensitive signalling, so that cytoskeletal rearrangement and mechanotransduction can be regulated by an external geometry-mediated chirality. Cytoskeletal re-organization and mechanotransduction play crucial roles in cell viability and differentiation94,95. Compared with left-handed ASGs, D-handedness promotes more efficient cell proliferation, spreading and migration37. Because chiral ASGs could provide a suitable environment for stem cell amplification, the evidence that the pluripotency and self-renewal of human mesenchymal stem cells are maintained better on D-ASGs is extremely important in the context of stem cell bioengineering. Moreover, genome-wide and high-throughput RNA sequencing analysis demonstrated that the effect of chirality on the regulation of stem cell fate was influencing the upregulation of transcription factors responsible for regulating gene expression, control differentiation, proliferation and apoptosis. However, more effort is needed to analyse the mechanistic functions of genes in stem cells regulated by one chiral form over the other. In another study, right-handed structured hydroxyapatite films on mica wafers showed some advantages in cell adhesion, cell proliferation and osteogenic differentiation of adipose-derived mesenchymal stem cells in comparison to the left-handed geometry, again showing that bioactive chiral patterns with proper handedness can enlarge cellular functions96. Therefore, chiral nanopatterns could be used as functional coatings on tissue engineering scaffolds or membrane materials to regulate cellular behaviours and differentiation for better tissue repair.

Outlook

Since 2018, intrinsically chiral engineered materials have begun to attract much more attention than their extrinsically chiral counterparts owing to their unique effects on various biological processes37,66,71. For this field to progress, advances will need to be made in several areas.

Preparation methods

Various strategies have been developed to prepare intrinsically chiral engineered materials. Chiral CDs and MBMs are generally prepared in the presence of chiral molecules with or without the assistance of physical stimuli, whereas patterned chiral geometries are most often made by photolithography. However, issues of versatility and reproducibility remain in the different methods.

On the basis of the available literature, chiral molecule-induced synthesis is the most versatile for constructing intrinsically chiral engineered materials, because the synthesis process is simple and can mass-produce materials. Polarized light-mediated synthesis introduces an alternative way to prepare chiral NPs, but it requires the implementation of a light transmission reaction system. Importantly, the uniformity of chiral NPs prepared by either chiral molecule-induced or polarized light-mediated synthesis is not yet satisfactory to reach high standards of precise reproducibility, which is a common problem in nanomaterial preparation. Furthermore, chiral molecule-induced synthesis seems unsuitable to construct chiral patterns or coatings on the surface of materials, unless the chiral nanostructures are able to grow on the surface of the substrates.

Photolithography is one of the most precise strategies to prepare chiral patterns or coatings with highly controlled parameters, but it usually costs high and is hard to scale up. It also cannot directly generate single chiral NPs. To address this issue, the combination of photolithography and demoulding processes may be a possible choice to prepare intrinsically chiral particles with precise and consistent parameters, but there is still a long way to implement this method.

Mechanisms of biological responses to chirality

For chiral CDs and MBMs, the interaction between the materials and biomolecules, cells or bacteria primarily determines any chiralitymediated biological effects21,31,34,69. Traditional antigen strategies have the shortcomings of low stability, side effects and high cost97. As potential antigen mimics, intrinsically chiral engineered nanomaterials usually can overcome these limitations, but suffer from a lack of targeting98.

Chirality can affect the affinity of a nanomaterial to biomolecules, cells and/or bacteria and thus its ability to regulate biomolecular functions and affect the behaviours of cells and bacteria. For instance, because L-handed metal NPs are internalized more efficiently by immune cells than D-handed NPs, they trigger a stronger immune response, making them promising engineered antigen mimetics for

antiviral and cancer therapies35,73. To rationally design chiral nanomaterials with desired affinity, however, thorough studies are required to understand the exact role of their chirality in the cellular signal pathway mechanisms.

By contrast, patterned chiral geometries mainly regulate cell fate by nanotopography-mediated modifications of the extracellular microenvironment, similar to the common regulatory mechanism of microstructure-induced or nanostructure-induced cell responses36,37,85,94. A deep understanding of the interaction between these geometries and cell fate will be important to build functional chiral coatings on the surface of biomaterials for stem cell and tissue engineering99,100.

Biotechnology strategies based on metabonomics, transcriptomics, proteomics, single-cell and gene sequencing have become powerful tools to investigate intracellular signal pathways. These tools will greatly help to elucidate the mechanisms of chirality-mediated biological responses. Moreover, it is well known that cell mechanical properties play an important role in cellular behaviours. New nanosensors that exploit atomic force microscopy and optical tweezers for single-cell mechanical interrogation are attracting attention in this context101,102 and are beginning to clearly clarify how chiral materials mediate the mechanotransduction process103,104.

Safety aspects

Crucially, intrinsically chiral materials carry safety concerns that need to be addressed. An alarm bell is the drug thalidomide tragedy, which neglected the severe side effects of the l-enantiomer105. Before engineered materials, especially nanomaterials, are translated to the clinic, they must be assessed to ensure that their intrinsic chirality has no long-term undesired health effects. In addition, similar to traditional biomaterials, the biocompatibility of chiral nanomaterials and chiral substrates cannot be neglected, especially for non-biodegradable or biopersistent materials and for materials liberating or generating toxic degradation by-products.

A bright future

Intrinsically chiral materials show great promise in different bioapplications. The ability of chiral engineered materials to change cellular uptake capacity can be used, for example, to control the specific delivery of drugs or genes. They are also hoped to influence tissue regeneration by regulating stem cell differentiation and to serve as new antimicrobials by efficiently inhibiting wound infection. Furthermore, chiral materials could serve as templates to construct chiral supramolecular assemblies by transferring their chiral information to achiral materials or molecules106. They may even be able to change the chirality of chiral biomolecules such as amino acids, proteins and DNA or chiral materials, thus changing their biological effects.

Building mirror-image biological systems is a fascinating area of research linked to the study of the origin of life. In this context, the mirror-image T7 RNA polymerase achieved the mirror-image T7 transcription of chirally inverted ribosomal and functional RNAs, which can be used for riboswitch sensing, long-term water storage of unprotected kilobase-long L-RNA and L-ribozyme-catalysed L-RNA polymerization23. It is interesting to investigate whether intrinsically chiral engineered materials, given their enzyme mimicking10 and chirality transfer properties106, can be used to construct chirally inverted biomacromolecules. This function would open new research directions towards (bio)applications, including designing and building mirror-image biological systems for bioorthogonal information storage107 and therapeutic protein formation108. Finally, being able to dynamically invert the chirality of engineered materials between L-handedness and D-handedness would provide the ability to meet the changing requirements of different biological stages in an on-demand way109, promoting the development of new intrinsically chiral smart materials.

Acknowledgements

Dedicated to the 70th birthday of M. Prato. The authors greatly acknowledge the financial support from the National Natural Science Foundation of China (No. 82100974), Shandong Province Key Research and Development Program (No. 2021ZDSYS18), Shandong Province Natural Science Foundation (No. ZR2021QH241), Young Elite Scientist Support Program by CSA (No. 2021PYRC001) and Qilu Young Scholars Program of Shandong University. This work was partly supported by the Interdisciplinary Thematic Institute SysChem via the IdEx Unistra (ANR-10-IDEX-0002) within the programme 'Investissement d'Avenir'. A.B. acknowledges the Centre National de la Recherche Scientifique and the International Center for Frontier Research in Chemistry.

Author contributions

B.M. and A.B. envisioned and prepared the Perspective article, carried out the literature survey, analysed the data, prepared the figures and wrote the paper.

Competing interests

The authors declare no competing interests.

References

1 Lv, J. *et al.* Self-assembled inorganic chiral superstructures. *Nat. Rev. Chem.* **6**, 125-145 (2022).

2 Mayoral, M. J. *et al.* Dual-mode chiral self-assembly of cone-shaped subphthalocyanine aromatics. *J. Am. Chem. Soc.* **142**, 21017–21031 (2020).

3 Parton, T. G. *et al.* Chiral self-assembly of cellulose nanocrystals is driven by crystallite bundles. *Nat. Commun.* **13**, 2657 (2022).
4 Shen, Z. *et al.* Asymmetric catalysis mediated by a mirror symmetry-broken helical nanoribbon. *Nat. Commun.* **10**, 3976 (2019).
5 Stolz, S. *et al.* Asymmetric elimination reaction on chiral metal surfaces. *Adv. Mater.* **34**, 2104481 (2022).
6 Liu, Z.-S. *et al.* Construction of axial chirality via palladium/chiral norbornene cooperative catalysis. *Nat. Catal.* **3**, 727-733 (2020).
7 Dong, K., Xu, C., Ren, J. & Qu, X. Chiral nanozymes for enantioselective biological catalysis. *Angew. Chem. Int. Ed.* **61**, e202208757 (2022).
8 Rosso, C., Filippini, G. & Prato, M. Carbon dots as nano-organocatalysts for synthetic applications. *ACS Catal.* **10**, 8090-8105 (2020).
9 Bai, T. *et al.* Chiral mesostructured NiO films with spin polarisation. *Angew. Chem. Int. Ed.* **60**, 9421–9426 (2021).
10 Li, F. *et al.* Chiral carbon dots mimicking topoisomerase I to mediate the topological rearrangement of supercoiled DNA enantioselectively. *Angew. Chem. Int. Ed.* **59**, 11087-11092 (2020).
11 Shao, Y. *et al.* Shining light on chiral inorganic nanomaterials for biological issues. *Theranostics* **11**, 9262-9295 (2021).
12 Hooftman, A. & O'Neill, L. A. Nanoparticle asymmetry shapes an immune response. *Nature* **601**, 323-325 (2022).
13 Lebreton, G. *et al.* Molecular to organismal chirality is induced by the conserved myosin 1D. *Science* **362**, 949-952 (2018).
14 Gao, R. *et al.* Site-selective proteolytic cleavage of plant viruses by photoactive chiral nanoparticles. *Nat. Catal.* **5**, 694–707 (2022).
15 Döring, A., Ushakova, E. & Rogach, A. L. Chiral carbon dots: synthesis, optical properties, and emerging applications. *Light Sci. Appl.* **11**, 1–23 (2022).
16 Zhang, N.-N. *et al.* Gold nanoparticle enantiomers and their chiral-morphology dependence of cellular uptake. *CCS Chem.* **4**, 660-670 (2022).
17 Ma, W. *et al.* Chiral inorganic nanostructures. *Chem. Rev.* **117**, 8041-8093 (2017).
18 Qu, S., Jia, Q., Li, Z., Wang, Z. & Shang, L. Chiral NIR-II fluorescent Ag_2S quantum dots with stereospecific biological interactions and tumor accumulation behaviors. *Sci. Bull.* **67**, 1274-1283 (2022).
19 Jia, T.-T. *et al.* Enantiomeric alkynyl-protected Au10 clusters with chirality-dependent radiotherapy enhancing effects. *Nano Today* **39**, 101222 (2021).
20 Tang, H., Li, Q., Yan, W. & Jiang, X. Reversing the chirality of surface ligands can improve the biosafety and pharmacokinetics of cationic gold nanoclusters. *Angew. Chem. Int. Ed.* **60**, 13829-13834 (2021).
21 Zhang, M., Zhang, H., Feng, J., Zhou, Y. & Wang, B. Synergistic chemotherapy, physiotherapy and photothermal therapy against bacterial and biofilms infections through construction of chiral glutamic acid functionalized gold nanobipyramids. *Chem. Eng. J.* **393**, 124778 (2020).
22 Wang, Z., Xu, W., Liu, L. & Zhu, T. F. A synthetic molecular system capable of mirror-image genetic replication and transcription. *Nat. Chem.* **8**, 698-704 (2016).
23 Xu, Y. & Zhu, T. F. Mirror-image T7 transcription of chirally inverted ribosomal and functional RNAs. *Science* **378**, 405-412 (2022).
24 Gal, J. Pasteur and the art of chirality. *Nat. Chem.* **9**, 604–605 (2017).
25 Zhou, C. *et al.* Chiral hierarchical structure of bone minerals. *Nano Res.* **15**, 1295-1302 (2022).

26 Jiang, W., Yi, X. & McKee, M. D. Chiral biomineralized structures and their biomimetic synthesis. *Mater. Horiz.* **6**, 1974-1990 (2019).
27 Kuroda, R., Endo, B., Abe, M. & Shimizu, M. Chiral blastomere arrangement dictates zygotic left–right asymmetry pathway in snails. *Nature* **462**, 790-794 (2009).
28 González-Rubio, G. *et al.* Micelle-directed chiral seeded growth on anisotropic gold nanocrystals. *Science* **368**, 1472–1477 (2020).
29 Lee, H.-E. *et al.* Cysteine-encoded chirality evolution in plasmonic rhombic dodecahedral gold nanoparticles. *Nat. Commun.* **11**, 263 (2020).
30 Jiang, W. *et al.* Emergence of complexity in hierarchically organized chiral particles. *Science* **368**, 642-648 (2020).
31 Zhang, M. *et al.* Chiral carbon dots derived from serine with well-defined structure and enantioselective catalytic activity. *Nano Lett.* **22**, 7203-7211 (2022).
32 Zhang, M. *et al.* Maltase decorated by chiral carbon dots with inhibited enzyme activity for glucose level control. *Small* **15**, 1901512 (2019).
33 Gao, P., Xie, Z. & Zheng, M. Chiral carbon dots-based nanosensors for Sn(II) detection and lysine enantiomers recognition. *Sens. Actuators B Chem.* **319**, 128265 (2020).
34 Shi, B. *et al.* Chiral nanoparticles force neural stem cell differentiation to alleviate Alzheimer's disease. *Adv. Sci.* **9**, 2202475 (2022).
35 Xu, L. *et al.* Enantiomer-dependent immunological response to chiral nanoparticles. *Nature* **601**, 366-373 (2022).
36 Yao, X., Wang, X. & Ding, J. Exploration of possible cell chirality using material techniques of surface patterning. *Acta Biomater.* **126**, 92-108 (2021).
37 Dong, L. *et al.* Chiral geometry regulates stem cell fate and activity. *Biomaterials* **222**, 119456 (2019).
38 Manoccio, M. *et al.* Femtomolar biodetection by a compact core-shell 3D chiral metamaterial. *Nano Lett.* **21**, 6179-6187 (2021).
39 Yuan, A. *et al.* Chiral Cu_xOS@ZIF-8 nanostructures for ultrasensitive quantification of hydrogen sulfide in vivo. *Adv. Mater.* **32**, 1906580 (2020).
40 Hao, C. *et al.* Chiral molecule-mediated porous Cu_xO nanoparticle clusters with antioxidation activity for ameliorating parkinson's disease. *J. Am. Chem. Soc.* **141**, 1091–1099 (2019).
41 Agnew-Francis, K. A. & Williams, C. M. Squaramides as bioisosteres in contemporary drug design. *Chem. Rev.* **120**, 11616–11650 (2020).
42 Holman, K. R., Stanko, A. M. & Reisman, S. E. Palladium-catalyzed cascade cyclizations involving C–C and C–X bond formation: strategic applications in natural product synthesis. *Chem. Soc. Rev.* **50**, 7891-7908 (2021).
43 Li, S. *et al.* The development of carbon dots: From the perspective of materials chemistry. *Mater. Today* **51**, 188-207 (2021).
44 Đorđević, L., Arcudi, F., Cacioppo, M. & Prato, M. A multifunctional chemical toolbox to engineer carbon dots for biomedical and energy applications. *Nat. Nanotechnol.* **17**, 112–130 (2022).
45 Đorđević, L., Arcudi, F. & Prato, M. Preparation, functionalization and characterization of engineered carbon nanodots. *Nat. Protoc.* **14**, 2931–2953 (2019).
46 Arcudi, F., Đorđević, L. & Prato, M. Design, synthesis, and functionalization strategies of tailored carbon nanodots. *Acc. Chem. Res.* **52**, 2070–2079 (2019).
47 Di Noja, S. *et al.* Transfer of axial chirality to the nanoscale endows carbon nanodots with circularly polarized luminescence. *Angew. Chem. Int. Ed.* **61**, e202202397 (2022).
48 Liu, Y. *et al.* Advances in carbon dots: from the perspective of traditional quantum dots. *Materials Chemistry Frontiers* **4**, 1586-1613 (2020).

49 Kang, Z. & Lee, S.-T. Carbon dots: advances in nanocarbon applications. *Nanoscale* **11**, 19214-19224 (2019).

50 Chen, Z., Liu, Y. & Kang, Z. Diversity and tailorability of photoelectrochemical properties of carbon dots. *Acc. Chem. Res.* **55**, 3110–3124 (2022).

51 Hutton, G. A. M., Martindale, B. C. M. & Reisner, E. Carbon dots as photosensitisers for solar-driven catalysis. *Chem. Soc. Rev.* **46**, 6111-6123 (2017).

52 Gao, W. *et al.* Deciphering the catalytic mechanism of superoxide dismutase activity of carbon dot nanozyme. *Nat. Commun.* **14**, 160 (2023).

53 d'Ischia, M., Napolitano, A., Ball, V., Chen, C.-T. & Buehler, M. J. Polydopamine and eumelanin: From structure-property relationships to a unified tailoring strategy. *Acc. Chem. Res.* **47**, 3541–3550 (2014).

54 Sun, M.-C. *et al.* Biomimetic melanosomes promote orientation-selective delivery and melanocyte pigmentation in the H_2O_2-induced vitiligo mouse model. *ACS Nano* **15**, 17361-17374 (2021).

55 Natarajan, V. T., Ganju, P., Ramkumar, A., Grover, R. & Gokhale, R. S. Multifaceted pathways protect human skin from UV radiation. *Nat. Chem. Biol.* **10**, 542-551 (2014).

56 Pommier, Y., Nussenzweig, A., Takeda, S. & Austin, C. Human topoisomerases and their roles in genome stability and organization. *Nat. Rev. Mol. Cell Biol.* **23**, 407-427 (2022).

57 Inzucchi, S. E. *et al.* Management of hyperglycemia in type 2 diabetes, 2015: a patient-centered approach: update to a position statement of the American Diabetes Association and the European Association for the Study of Diabetes. *Diabetes Care* **38**, 140-149 (2015).

58 Umpierrez, G. E. & Pasquel, F. J. Management of inpatient hyperglycemia and diabetes in older adults. *Diabetes Care* **40**, 509-517 (2017).

59 Lingvay, I., Sumithran, P., Cohen, R. V. & le Roux, C. W. Obesity management as a primary treatment goal for type 2 diabetes: time to reframe the conversation. *The Lancet* **399**, 394-405 (2022).

60 Ahmad, E., Lim, S., Lamptey, R., Webb, D. R. & Davies, M. J. Type 2 diabetes. *The Lancet* **400**, 1803–1820 (2022).

61 Rines, A. K., Sharabi, K., Tavares, C. D. J. & Puigserver, P. Targeting hepatic glucose metabolism in the treatment of type 2 diabetes. *Nat. Rev. Drug Discov.* **15**, 786-804 (2016).

62 Cao, M. *et al.* Molybdenum derived from nanomaterials incorporates into molybdenum enzymes and affects their activities in vivo. *Nat. Nanotechnol.* **16**, 708–716 (2021).

63 Ren, J. *et al.* Chemical and biophysical signatures of the protein corona in nanomedicine. *J. Am. Chem. Soc.* **144**, 9184-9205 (2022).

64 Yan, H. *et al.* Influence of the chirality of carbon nanodots on their interaction with proteins and cells. *Nat. Commun.* **12**, 7208 (2021).

65 Mosquera, J. *et al.* Reversible control of protein corona formation on gold nanoparticles using host-guest interactions. *ACS Nano* **14**, 5382-5391 (2020).

66 Li, F. *et al.* Highly fluorescent chiral N-S-doped carbon dots from cysteine: Affecting cellular energy metabolism. *Angew. Chem. Int. Ed.* **57**, 2377-2382 (2018).

67 Ma, Y. *et al.* Chiral carbon dots-a functional domain for tyrosinase Cu active site modulation via remote target interaction. *Nanoscale* **14**, 1202-1210 (2022).

68 Zhang, M. *et al.* Chiral control of carbon dots via surface modification for tuning the enzymatic activity of glucose oxidase. *ACS Appl. Mater. Interfaces* **13**, 5877-5886 (2021).

69 Gao, P. *et al.* Chiral carbon dots-enzyme nanoreactors with enhanced catalytic activity for cancer therapy. *ACS Appl. Mater. Interfaces* **13**, 56456–56464 (2021).

70 Liu, H., Xie, Z. & Zheng, M. Unprecedented Chiral Nanovaccines for Significantly Enhanced Cancer Immunotherapy. *ACS Appl. Mater. Interfaces* **14**, 39858-39865 (2022).
71 Zhang, M. *et al.* One-step hydrothermal synthesis of chiral carbon dots and their effects on mung bean plant growth. *Nanoscale* **10**, 12734-12742 (2018).
72 Victoria, F., Manioudakis, J., Zaroubi, L., Findlay, B. & Naccache, R. Tuning residual chirality in carbon dots with anti-microbial properties. *RSC Adv.* **10**, 32202-32210 (2020).
73 Wang, W. *et al.* The development of chiral nanoparticles to target NK cells and $CD8^+$ T cells for cancer immunotherapy. *Adv. Mater.* **34**, 2109354 (2022).
74 Lee, H.-E. *et al.* Amino-acid-and peptide-directed synthesis of chiral plasmonic gold nanoparticles. *Nature* **556**, 360-365 (2018).
75 Ma, Y. *et al.* Controlled synthesis of Au chiral propellers from seeded growth of Au nanoplates for chiral differentiation of biomolecules. *J. Phys. Chem. C* **124**, 24306-24314 (2020).
76 Qu, A. *et al.* Stimulation of neural stem cell differentiation by circularly polarized light transduced by chiral nanoassemblies. *Nat. Biomed. Eng.* **5**, 103-113 (2021).
77 Poewe, W. *et al.* Parkinson disease. *Nat. Rev. Dis. Primers* **3**, 17013 (2017).
78 Shi, B. *et al.* Chiral Cu_xCo_yS supraparticles ameliorate parkinson's disease. *CCS Chem.* **4**, 2440-2451 (2022).
79 Chen, P. *et al.* Peptide-directed synthesis of chiral nano-bipyramids for controllable antibacterial application. *Chem. Sci.* **13**, 10281-10290 (2022).
80 Wang, G. *et al.* Six-pointed star chiral cobalt superstructures with strong antibacterial activity. *Small* **18**, 2204219 (2022).
81 Liu, Z. *et al.* Nano-kirigami with giant optical chirality. *Sci. Adv.* **4**, eaat4436 (2018).
82 Wei, X. *et al.* Enantioselective photoinduced cyclodimerization of a prochiral anthracene derivative adsorbed on helical metal nanostructures. *Nat. Chem.* **12**, 551-559 (2020).
83 Palermo, G. *et al.* Biomolecular sensing at the interface between chiral metasurfaces and hyperbolic metamaterials. *ACS Appl. Mater. Interfaces* **12**, 30181-30188 (2020).
84 García-Guirado, J., Svedendahl, M., Puigdollers, J. & Quidant, R. Enantiomer-selective molecular sensing using racemic nanoplasmonic arrays. *Nano Lett.* **18**, 6279–6285 (2018).
85 Elnathan, R. *et al.* Biointerface design for vertical nanoprobes. *Nat. Rev. Mater.* **7**, 953–973 (2022).
86 Yao, X., Hu, Y., Cao, B., Peng, R. & Ding, J. Effects of surface molecular chirality on adhesion and differentiation of stem cells. *Biomaterials* **34**, 9001-9009 (2013).
87 Peng, Y. *et al.* Degradation rate affords a dynamic cue to regulate stem cells beyond varied matrix stiffness. *Biomaterials* **178**, 467-480 (2018).
88 Ye, K. *et al.* Matrix stiffness and nanoscale spatial organization of cell-adhesive ligands direct stem cell fate. *Nano Lett.* **15**, 4720-4729 (2015).
89 Tang, J., Peng, R. & Ding, J. The regulation of stem cell differentiation by cell-cell contact on micropatterned material surfaces. *Biomaterials* **31**, 2470-2476 (2010).
90 Yao, X., Peng, R. & Ding, J. Cell-material interactions revealed via material techniques of surface patterning. *Adv. Mater.* **25**, 5257-5286 (2013).
91 Wang, Y. *et al.* Micropattern-controlled chirality of focal adhesions regulates the cytoskeletal arrangement and gene transfection of mesenchymal stem cells. *Biomaterials* **271**, 120751 (2021).
92 Yao, X. & Ding, J. Effects of microstripe geometry on guided cell migration. *ACS Appl. Mater. Interfaces* **12**, 27971-27983 (2020).

93 Zhang, J. *et al.* The osteogenic response to chirality-patterned surface potential distribution of CFO/P(VDF-TrFE) membranes. *Biomater. Sci.* **10**, 4576-4587 (2022).
94 von Erlach, T. C. *et al.* Cell-geometry-dependent changes in plasma membrane order direct stem cell signalling and fate. *Nat. Mater.* **17**, 237-242 (2018).
95 Murphy, W. L., McDevitt, T. C. & Engler, A. J. Materials as stem cell regulators. *Nat. Mater.* **13**, 547-557 (2014).
96 Zhou, C. *et al.* Enantioselective interaction between cells and chiral hydroxyapatite films. *Chem. Mater.* **34**, 53-62 (2022).
97 Hansel, T. T., Kropshofer, H., Singer, T., Mitchell, J. A. & George, A. J. T. The safety and side effects of monoclonal antibodies. *Nat. Rev. Drug Discov.* **9**, 325–338 (2010).
98 Scott, A. M., Wolchok, J. D. & Old, L. J. Antibody therapy of cancer. *Nat. Rev. Cancer* **12**, 278-287 (2012).
99 Kong, Y. *et al.* Regulation of stem cell fate using nanostructure-mediated physical signals. *Chem. Soc. Rev.* **50**, 12828-12872 (2021).
100 Wan, X., Liu, Z. & Li, L. Manipulation of stem cells fates: The master and multifaceted roles of biophysical cues of biomaterials. *Adv. Funct. Mater.* **31**, 2010626 (2021).
101 Hao, Y. *et al.* Mechanical properties of single cells: Measurement methods and applications. *Biotechnol. Adv.* **45**, 107648 (2020).
102 Hang, X. *et al.* Nanosensors for single cell mechanical interrogation. *Biosens. Bioelectn.* **179**, 113086 (2021).
103 Finbloom, J. A., Huynh, C., Huang, X. & Desai, T. A. Bioinspired nanotopographical design of drug delivery systems. *Nat. Rev. Bioeng.* **1**, 139–152 (2023).
104 Sun, L. *et al.* Ultrastructural organization of NompC in the mechanoreceptive organelle of Drosophila campaniform mechanoreceptors. *Proc. Natl. Acad. Sci. U.S.A.* **116**, 7343-7352 (2019).
105 Franks, M. E., Macpherson, G. R. & Figg, W. D. Thalidomide. *The Lancet* **363**, 1802–1811 (2004).
106 Đorđević, L. *et al.* Design principles of chiral carbon nanodots help convey chirality from molecular to nanoscale level. *Nat. Commun.* **9**, 3442 (2018).
107 Fan, C., Deng, Q. & Zhu, T. F. Bioorthogonal information storage in l-DNA with a high-fidelity mirror-image *Pfu* DNA polymerase. *Nat. Biotechnol.* **39**, 1548-1555 (2021).
108 Weidmann, J., Schnölzer, M., Dawson, P. E. & Hoheisel, J. D. Copying life: Synthesis of an enzymatically active mirror-image DNA-ligase made of d-amino acids. *Cell Chem. Biol.* **26**, 645-651.e643 (2019).
109 Park, J. E. *et al.* On-demand dynamic chirality selection in flower corolla-like micropillar arrays. *ACS Nano* **16**, 18101-18109 (2022).